Magnetic susceptibility and facies relationship in Bajocian–Bathonian carbonates from the Azé caves, southeastern Paris Basin, France

S. DECHAMPS*, A. C. DA SILVA & F. BOULVAIN

Sedimentary Petrology, B20, University of Liège, Sart-Tilman, 4000 Liège, Belgium

**Corresponding author (e-mail: s.dechamps@doct.ulg.ac.be)*

Abstract: This study focuses on three Bajocian and Bathonian carbonate sections from the southeastern part of the Paris Basin (Mâconnais area, in the east of France). The main goals of the study are to propose a palaeoenvironmental model, to get insight into vertical and lateral facies evolution, to improve correlations and to better understand the origin of the magnetic susceptibility (MS) signal in these deposits. The sedimentological setting corresponds to a ramp, with two types of geometries: (1) a homoclinal carbonate ramp with oolitic shoals; and (2) a multiple-slopes carbonate ramp with reef complexes. The MS signal appears to be influenced by facies and ramp geometry. The evolution of MS seems to be mainly related to changes in carbonate productivity and water agitation: oolitic facies and reef complexes, with high carbonate production show the lowest signal, while storm deposits are characterized by higher values. In addition, the MS signal from proximal tempestites have higher values than distal ones. MS appears to be a useful complementary proxy for palaeoenvironmental interpretations, correlations and sequential stratigraphy. The facies evolution, supported by MS curves, shows at least nine successive depositional sequences, which were inserted into the regional sequential canvas.

During the Aalenian–Bajocian transition, the Burgundy area experienced major changes in palaeogeography and biosedimentary domains (Contini & Mangold 1980; Durlet *et al.* 1997; Pellenard *et al.* 1998) due to the reactivation of Hercynian faults during the Mid Cimmerian tectonic event (Rat *et al.* 1986; Ziegler 1988). Coeval to the tectonic instability, a generic diversification of Scleractinia occurred, and these corals became the main frame-builders in reefs (Lathuilière & Marchal 2009). This predates the basin-scale expansion of the carbonate platform during the Middle Jurassic (Dercourt *et al.* 1993). The climatic transition from warm and moist conditions during the Lower Bajocian to cooler and dryer conditions during the Upper Bajocian (Hesselbo *et al.* 2003; Dera *et al.* 2011) affected seawater chemistry, carbonate productivity and the growth dynamics of reefs (Dromart *et al.* 1996; Gibbs *et al.* 1999; Piuz 2004; Brigaud *et al.* 2009). However, despite these major changes, the sedimentology of the Mâconnais area is still largely unknown and fundamental questions concerning matters such as the stratigraphic and sequential correlations at small and regional scale, and the geometry of the platform, have still to be answered. For this work, the reference section is the Saint-Gengoux-de-Scissé (SGS) section, an exceptionally long and continuous section for the Bajocian and Bathonian of Burgundy (Pellenard *et al.* 1998). It shows noticeable lithological differences from the regional Bajocian and Bathonian series (Perthuisot 1966; Barusseau 1967; Purser 1975; Pellenard *et al.* 1998). We also selected two sections in the Azé caves (Grotte Préhistorique, Grotte de la Rivière). Despite the good quality of the outcrops (Barriquand & Barriquand 2000, 2001, 2009; Combier *et al.* 2000; Barriquand *et al.* 2006) the Bajocian and Bathonian of the Azé caves have never been subject to an extensive sedimentological study.

In order to develop a better insight into the sedimentary dynamics and palaeoenvironmental evolution during the Bajocian and Bathonian of the southeastern Paris Basin, we have applied classic sedimentological study methods and sequence stratigraphy, as well as magnetic susceptibility (MS) measurements through the different sections. This methodology has allowed us to: (1) increase precision over the lithostratigraphy canvas for the Bajocian and Bathonian of the Mâconnais; (2) build a sedimentological model for the Middle Jurassic of the Mâconnais; (3) integrate the sections in a regional sequential framework; and (4) test the use of MS as a correlation tool and as a proxy for palaeoenvironmental variations.

Since the end of the 1990s, the use of MS in sedimentology has become common (Crick *et al.* 1997, 2000, 2001, 2002; Ellwood *et al.* 1999, 2000, 2001). Widely used on Palaeozoic or Mesozoic rocks, MS analyses allow high resolution stratigraphic correlations and helps with the interpretation of

From: Da Silva, A. C., Whalen, M. T., Hladil, J., Chadimova, L., Chen, D., Spassov, S., Boulvain, F. & Devleeschouwer, X. (eds) 2015. *Magnetic Susceptibility Application: A Window onto Ancient Environments and Climatic Variations*. Geological Society, London, Special Publications, **414**, 93–109.
First published online March 23, 2015, http://doi.org/10.1144/SP414.11

depositional dynamics and environments (Ellwood *et al.* 2001, 2006, 2007, 2013; Da Silva & Boulvain 2002, 2003, 2006; Whalen & Day 2008; Boulvain *et al.* 2010; Koptíková 2011). It is used as a proxy for sea-level changes (Crick *et al.* 1997, 2001; Devleeschouwer 1999; Ellwood *et al.* 2000; Zhang *et al.* 2000; Racki *et al.* 2002; Da Silva & Boulvain 2002, 2010; Da Silva *et al.* 2010; Hladil *et al.* 2003, 2005; Mabille & Boulvain 2007; Whalen & Day 2008, 2010) and/or climatic variations and for cyclostratigraphy (Ellwood *et al.* 2011, 2012; Boulila *et al.* 2008, 2010; De Vleeschouwer *et al.* 2012*a*, *b*; Da Silva *et al.* 2013). In this paper, MS is applied for the first time on the Bajocian and Bathonian from the Paris Basin. In order to use MS for palaeoenvironmental interpretation and to enhance the precision of correlation, we compared MS trends with facies. This also permits a better insight into the sedimentary dynamics of the platform and of the distribution of siliciclastic inputs within the different facies.

Geological setting

The studied area is located in the Mâconnais Mountains, which are in the southern part of the Saône-et-Loire department of Burgundy (France), 15 km NNW of Mâcon. The cuesta morphology of the Mâconnais Mountains is due to five SSW–NNE monoclinal ranges, separated by normal faults (Fig. 1). These are attributable to the Bresse Basin collapse during the Alpine compression (Perthuisot 1966; Rat *et al.* 1986). During the Bajocian and Bathonian, the intracratonic Paris Basin was covered by a shallow epicontinental sea (Ziegler 1988, Thierry 2000). The Mâconnais area was located at latitude 25–30° N and acted as a shallow connection between the central part of the Paris Basin and the Tethys Sea. A warm climate and a slow rate of subsidence, among other factors, allowed the development of a widespread carbonated platform (Purser 1975; Enay & Mangold 1980; Floquet *et al.* 1989; Durlet & Thierry 2000).

During the Aalenian, the area that is now Burgundy experienced a stage of tectonic instability coeval with a second-order regression maximum (Ziegler 1988; Dercourt *et al.* 1993; Graciansky *et al.* 1993; Jacquin *et al.* 1998; Hallam 2001). A major part of the platform was exposed, leading to the development of the Mid Cimmerian unconformity (Ziegler 1988). The first Bajocian Formation which lies on top of the Mid Cimmerian disconformity (Purser 1975; Morestin 1986; Ziegler 1988) is the Calcaire à Entroques Formation, a widespread unit composed of crinoidal limestones (Perthuisot 1966; Purser 1975; Benyahia 1982). Scleratinian biostromes and bioherms are classically observed in this Formation (Barusseau 1967; Purser 1975), corresponding to the Calcaire à Polypiers Member. This coral reef unit developed during the Lower Bajocian, in relation to the transgressive evolution which ended at the Vesulian disconformity. This surface highlights the maximum of regression of a high-amplitude third-order sequence leading to a regional emersion of the platform, emphasized by a hardened, burrowed and encrusted surface (Purser 1975; Durlet 1996). The Upper Bajocian records the end of the second-order transgressive phase (Jacquin *et al.* 1998; Hallam 2001) (Fig. 2), and the following regressive phase is coeval with the deposit of the Oolithe Blanche Formation (Purser 1975; Ferry *et al.* 2007), due to the renewal of the carbonate factory (Purser 1975; Dromart *et al.* 1996; Dera *et al.* 2011).

In the Upper Bajocian, several main formations can be identified: in succession, these are the Calcaire Grumeleux, the Marnes à *Ostrea acuminata*, and the Calcaire de Sermizelles Formations (Tintant 1963; Pellenard *et al.* 1998). However, these formations exhibit strong lateral variations in lithology (Durlet & Thierry 2000), and in our study area some of these formations have not been recognized.

The Bajocian–Bathonian boundary is highlighted by a progressive transition to oolitic limestones of the Oolithe Blanche Formation (Perthuisot 1966; Floquet *et al.* 1989; Pellenard *et al.* 1998).

We have selected a reference section at SGS (Fig. 2), which is the longest of the area. This section goes through the Rochebin Mountain along a west–east water adduction tunnel, 2.3 km north of the opening of the Azé caves. The west entrance is located at 46° 27′ 38″ N, 4° 45′ 34″ E, the east entrance at 46° 27′ 39″ N, 4° 46′ 59″ E. Only the eastern half of the 530 m-long tunnel has been described, as a fault repeats the series. This 87 m-thick section can be used as a framework for comparison with smaller sections: the Grotte Préhistorique section (46° 26′ 24″ N, 4° 45′ 40.5″ E, composite section visually correlated; Fig. 2) and the Grotte de la Rivière section (46° 26′ 23″ N, 4° 45′ 36. 5″ E, Fig. 2), both located in the karstic system reaching into the Rochebin Mountain (Berger & Martin 1995; Barriquand *et al*. 2006).

Methodology

Form the studied sections, 226 samples were collected for both thin-section and MS measurements. MS measurements were performed on the same samples as those used for the thin sections, in order to support the correlations, make direct comparison with facies trends, and support depositional interpretations. The analyses were performed on a

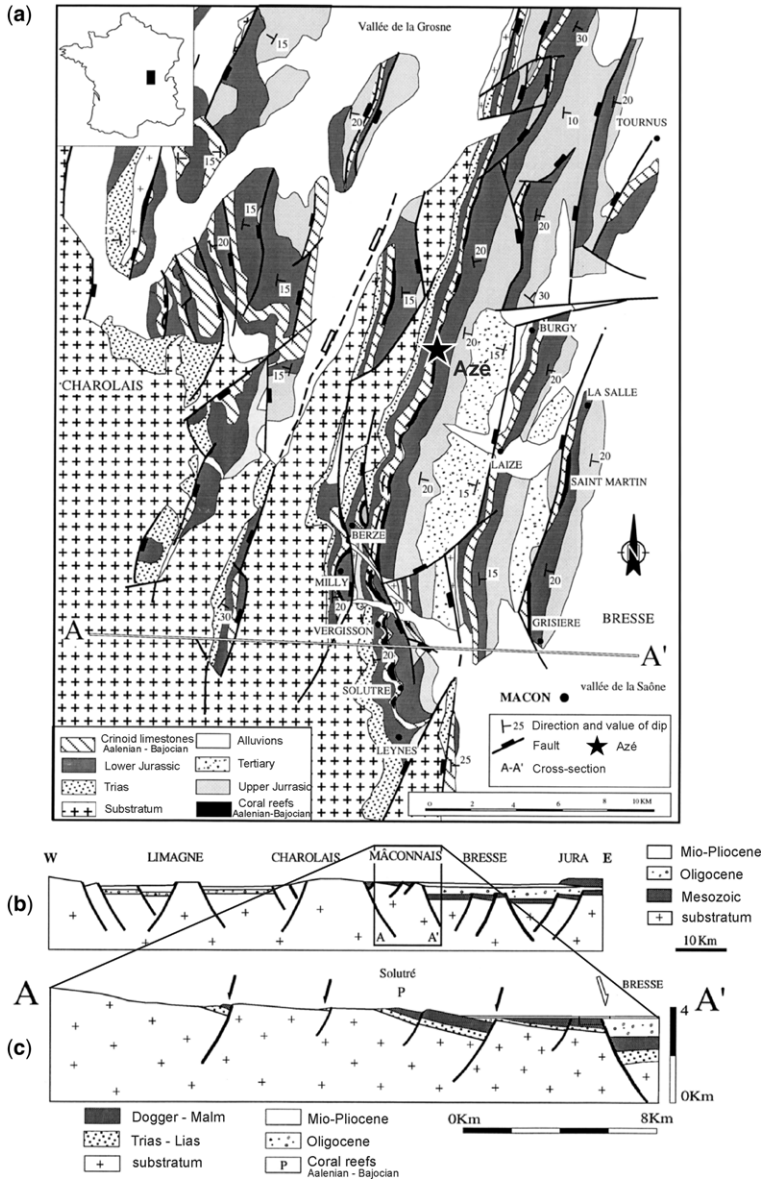

Fig. 1. (**a**) Localization of Azé in a simplified geological map of the Mâconnais Mountains area. Top section beneath map (**b**) is a west–east section through the eastern part of the Paris Basin; bottom section (**c**) is an expanded section of the Mâconnais Mountains area. The A–A′ transect is reported on the geological map (modified after Quesne *et al.* 2000).

KLY3 Kappabridge device at the University of Liège, where samples had been previously weighed with a 0.01 g precision. The displayed value for each sample is an average of three measurements and is expressed in $m^3\ kg^{-1}$. MS measurements vary with the nature, amount and grain size of the minerals.

Results

Description of the studied sections

As a reference section, the SGS section is the only one described in detail (for more information on other locations, see Fig. 2). The allocation to

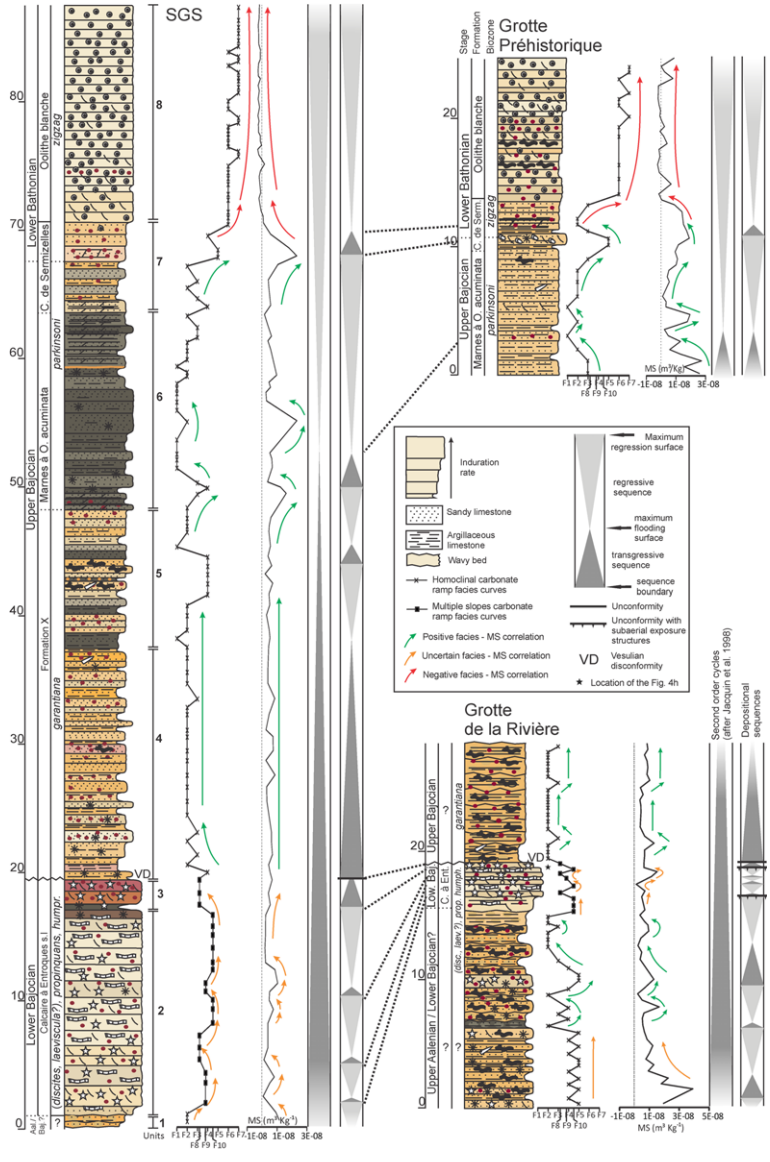

Fig. 2. Synthetized logs of the Saint-Gengoux-de-Scissé (SGS), Grotte de la Rivière and Grotte Préhistorique sections. Each section is presented with facies and magnetic susceptibility (MS) curves. Arrows highlight the MS and facies trends, and their colour illustrates the correlation between the two proxies (see legend). The second-order cycles are synthetized from Jacquin *et al.* (1998). Depositional sequences and correlations between logs are established on the basis of field work and facies, and supported by MS trends. The figured components are described in the legend for Figure 3.

existing formations is inferred on the basis of facies (e.g. Perthuisot 1966; Purser 1975; Pellenard *et al.* 1998). The chronostratigraphic and biostratigraphic frameworks of these formations (e.g. Pellenard *et al.* 1998; Durlet & Thierry 2000) have been used to date our sections.

Eight lithological units were defined (Fig. 2). Unit 1 (0–1.2 m) starts with yellowish marls, then nodular or wavy greenish silty limestones to calcareous marls. Except for sparse crinoids or pelecypods, this unit is lacking macro-fossils. The bed surfaces show red ribbons of metallic oxides.

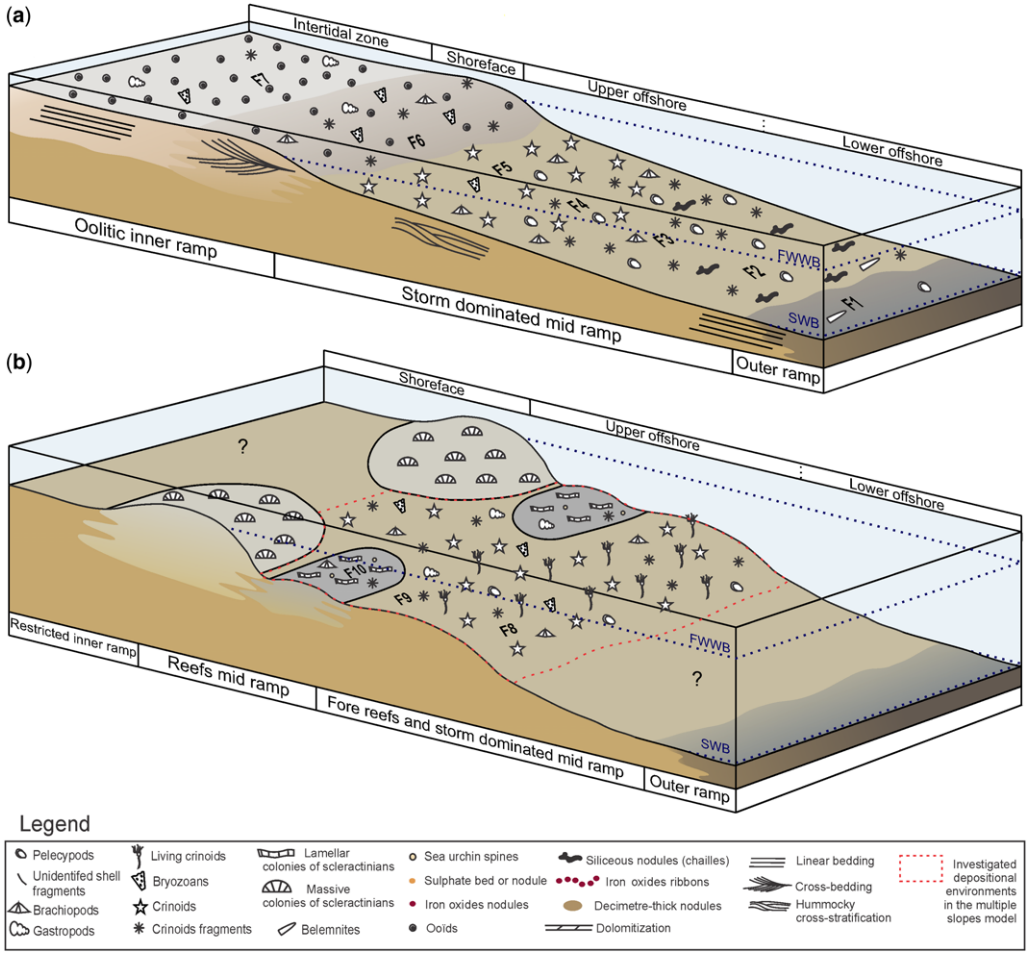

Fig. 3. (**a**) Carbonate ramp defined from F1 to F7 facies associations. The outer ramp (F1) marls were deposited under calm hemipelagic sedimentation. From the lower mid ramp (F2) to the upper mid ramp (F5), the biological productivity was higher, with frequent bioturbation and a predominantly coarse bioclastic fraction. The inner ramp (F6 and F7) is dominated by the action of tide and fair-weather waves, generating a prograding shoal. (**b**) Complex multiple-slopes carbonate ramp model defined from the F8 and F9–F10 facies associations. This model highlights the competition between crinoids and biostromes, and their spatial relationship with shallower and protecting bioherms. The figured elements are described in the legend. FWWB, fair weather wave base; SWB, storm wave base.

Unit 2 (1.2–16.8 m, corresponding to the Calcaire à Polypiers Member, included in the Calcaire à Entroques Formation), is a massive unit composed of greyish coral limestone (fine bioturbated limestone bearing lamellar recrystallized colonies) alternating with ochre bioclastic limestones (mainly composed of crinoids, shells fragments and reddish pigments). Unit 3 (16.8–19.2 m, corresponding to the upper Calcaire à Entroques Formation), is a blackish, brown, ochre, reddish or whitish coarse crinoidal limestones, with sparse shell fragments followed by coral limestones. For units 4–5, no correspondence with an existing formation was observed, so we have used the term 'Formation X'. Unit 4 (19.2–37.1 m, Formation X, Upper Bajocian) is composed of wavy sandy limestone and marl beds, mostly yellowish or ochre, to greyish for the more calcareous beds. Except for sparse crinoids or shells fragments, macro-fossils are scarce and siliceous nodules are common. Unit 5 (37.1–47.9 m, Formation X, Upper Bajocian) differs from the previous unit because of the appearance of several darker to black beds among the ochre beds (probably associated with organic matter, as

indicated by sulphate layers due to oxidation of pyrite). These beds contain only sparse belemnites. Unit 6 (47.9–63.2 m, a possible lateral equivalent of the Marnes à *O. acuminata* Formation) exposes black to dark-grey planar decimetric marls and pluridecimetric silty or sandy limestones, with a few centimetric sulphate layers. Apart from the strongly dolomitized lowest 2 m which have numerous crinoids, the scarce macro-fossils are dominated by plurimillimetric crinoids and recrystallized shells. Unit 7 (63.2–70.1 m, possible lateral equivalent of the Calcaire de Sermizelles Formation) is composed of ochre to reddish or greyish argillaceous and silty limestones. Unit 8 (70.1–87 m, corresponding to Oolithe Blanche Formation) shows a base composed of slightly silty and argillaceous pale-ochre limestones, followed by ooïds with crinoid-fragment limestones.

Facies

The sedimentological and petrographical descriptions of each facies are presented in Table 1.

In the following text, interpretations are highlighted for each facies, organized from the most distal to the most proximal for each model (Fig. 3).

Homoclinal carbonate ramp

F1: silty black marls. The mudstone texture, the clay fraction and organic matter conservation, the laminar bedding or lack of sedimentary structure, and the lack of bioturbation suggest a calm anoxic environment. The fauna, dominated by pelagic organisms such as belemnites, *Labalina* foraminifera (Piuz 2004), crinoid debris and bivalves, suggests an open-shelf environment.

F1 is interpreted as deposited in a calm disoxic to anoxic offshore environment, below the storm-wave base (Burchette & Wright 1992).

F2: silty marls with oxide ribbons, and F3: sandy marls with silicification. For both F2 and F3 facies, the wackestone texture, the clay and silt content, the low organic matter content, and the common planar bedding suggest a calm environment. The peloids, the occurrence of slightly wavy beddings, the alignment of grains and the laminae enriched in micritized bioclasts suggest short periods of increased agitation (Fig. 4a). The occurrence of siliceous nodules in these rocks has been described as related to *Thalassinoïdes* ichnofossils, produced by the silicification of crustacean burrows (Coulon 1979; Benyahia 1982). This hypothesis is supported here by their constant diameter (*c.* 3 cm) and their arborescent shape. Their concentration is higher in the F3 facies than in the F2, perhaps due to better oxygenation of the sediment or the smaller clay fraction. The fauna is dominated by belemnites, foraminifera, crinoids, bivalves and brachiopod debris, which suggest an open-shelf environment.

A calm lower offshore depositional environment, close to the storm-wave base and periodically agitated by distal storms, is proposed for the F2 and F3 facies (Tucker & Wright 1990; Burchette & Wright 1992); F2 was probably deposited in a slightly deeper setting than the F3 facies. The transition from disoxic (F2) to oxic (F3) conditions is coeval with the appearance of plurimillimetric laminae of coarser biodetrital inputs and lighter colours, and certainly suggests periods of gentle water agitation and water exchange due to storm waves.

F4: slightly detrital bioclastic limestone, and F5: bioclastic limestone. The widespread grainstone and packstone textures and the sorting and erosion of grains indicate a regularly agitated palaeoenvironment. Clay and coarser quartz inputs are diluted by the more efficient carbonate factory. In the field, facies are organized in fining-upward sequences and exhibit hummocky cross-stratifications and tabular cross-stratifications. Bioturbation and light colours attest to good oxygenation. The decrease in pelagic foraminifera and bivalves, substituted by crinoids and brachiopods, could be related to shallower conditions (Fig. 4b).

A storm-dominated upper offshore depositional environment is interpreted for the F4 and F5 facies. F5 facies has been strongly influenced by biodetrital supply reworked by storms, in conjunction with higher *in situ* carbonate production. F4 facies is considered to have been deposited in a slightly deeper and calmer setting.

F6: bioclastic–oolitic limestone, and F7: oolitic limestone. The grainstone texture, the abundance of oolitic grains, the absence of detrital elements (Fig. 4c), and the cross-bedding suggest a constantly agitated environment with high hydrodynamic conditions, above the fair-weather base. The presence of encrusting worms and *Codiacea* attests to good oxygenation conditions in a shallow environment located in the photic zone.

A shallow and constantly agitated shore environment is proposed (Purser 1975). The F6 facies was deposited in an upper shoreface environment in which oolitic grains mixed with *in situ* bioclastic materials accumulated. The F7 facies is consistent with a foreshore environment, where the fair-weather and tidal currents allowed the formation of ubiquitous α-ooïds (Purser 1975; Vincent *et al.* 1997).

Multiple-slopes carbonate ramp with bioconstructions

F8: crinoidal limestone. The generalized grainstone texture, coarser grains and common

Table 1. *Lithofacies and microfacies descriptions, and general environmental interpretations*

Lithofacies	Colour	Texture*	Bioclastic components†	Non-bioclastic components	Sedimentary and biogenic structures	Grain size and sorting	General Environmental Interpretation
Homoclinal Ramp							
F1 – silty black marls	Black to dark grey	Mudstone	Pelagic foraminifers, calcispheres, bivalves, crinoids	Quartz, clay, peloids, organic matter, oxide ribbons	Bioturbation, planar-bedding, siliceous nodules	Quartz: 10–100 μm VGS	Lower off-shore, below the storm waves base
F2 – silty marls with oxides ribbons	Ochre to grey	Wackestone	Pelagic foraminifers, bivalves, crinoids, calcispheres	Quartz, clay, peloids, organic matter (scarce), oxide ribbons	Bioturbation, planar (or wavy) bedding, nodular	200 μm to 1.5 mm Quartz: 50–100 μm GS	Lower off-shore, above thestorm waves base
F3 – sandy marls with silicifications	Ochre	Packstone	Microbioclasts, bivalves or crinoids fragments	Quartz, clay, peloids, oxide ribbons	Bioturbation, planar or wavy bedding, nodular	200 μm to 2 mm Quartz: 50–150 μm GS to MS	
F4 – slightly detrital bioclastic limestone	Pale ochre	Packstone/grainstone	Crinoids, bivalves, bryozoans, brachiopods, pelagic foraminifers	Quartz, clay, peloids, oxide ribbons or pigments	Bioturbation, planar or HCS stratification	500 μm to 4 mm Quartz: 100–150 μm MS to GS	Upper off-shore, storm-dominated
F5 – bioclastic limestone	Pale ochre to pale grey	Grainstone/packstone	Crinoids, brachiopods, bryozoans, bivalves	Quartz, clay, lumps, oxide pigments	Bioturbation, planar or HCS stratification	500 μm to >1 cm Quartz: 100–200 μm MS	
F6 – bio-oolitic limestone	Whitish to pale ochre	Grainstone	Crinoids, bryozoans, brachiopods, green algae, encrusting worms, foraminifers	Pseudo-ooïds, α and β-ooïds, mud-coated grains,	Planar-bedding, cross-bedding	300 μm to 4 mm MS to WS	Foreshore, above fair-weather base
F7 – oolitic limestone	White	Grainstone	Crinoids, brachiopods, gastropods, bryozoans, encrusting worms, foraminifers	α and β ooïds, mud-coated grains, lumps	Planar-bedding, tabular cross-bedding, HBS, stylolithic joints	500 μm to 1 mm MS to GS	Foreshore, tide domintaed
Multiple-slopes ramp							
F8 – crinoidal limestone	Grey ochre, reddish, pale ochre	Grainstone/packstone	Crinoids, brachiopods, gastropods, bryozoans, bivalves, foraminifers	Oxide pigments	Cross-bedding, planar-bedding, or no bedding	500 μm to 4 mm GS	Upper off-shore, storm-dominated
F9 – reefal bioclastic limestone	Pale ochre, grey ochre	Packstone/grainstone	Crinoids, brachiopods, gastropods, bivalves, urchin spines, corals fragments, bryozoans	Oxide pigments	No bedding, planar-bedding, or cross-bedding	500 μm to 5 mm GS to MS	Upper off-shore, below fair-weather waves base
F10 – coral limestone	Pale grey to grey	Framestone	Corals, urchin spines, crinoids, gastropods, brachiopods, bivalves	Slightly argillaceous	Biostrome, bioturbation	1 mm to >1 cm MS to WS	

*The textural classification of microfacies follows Dunham (1962).
†Bioclastic components are sorted in decreasing relative abundance: GS, good sorting; HCS, hummocky cross-stratifications; MS, moderate sorting; VGS, very good sorting; WS, weak sorting.

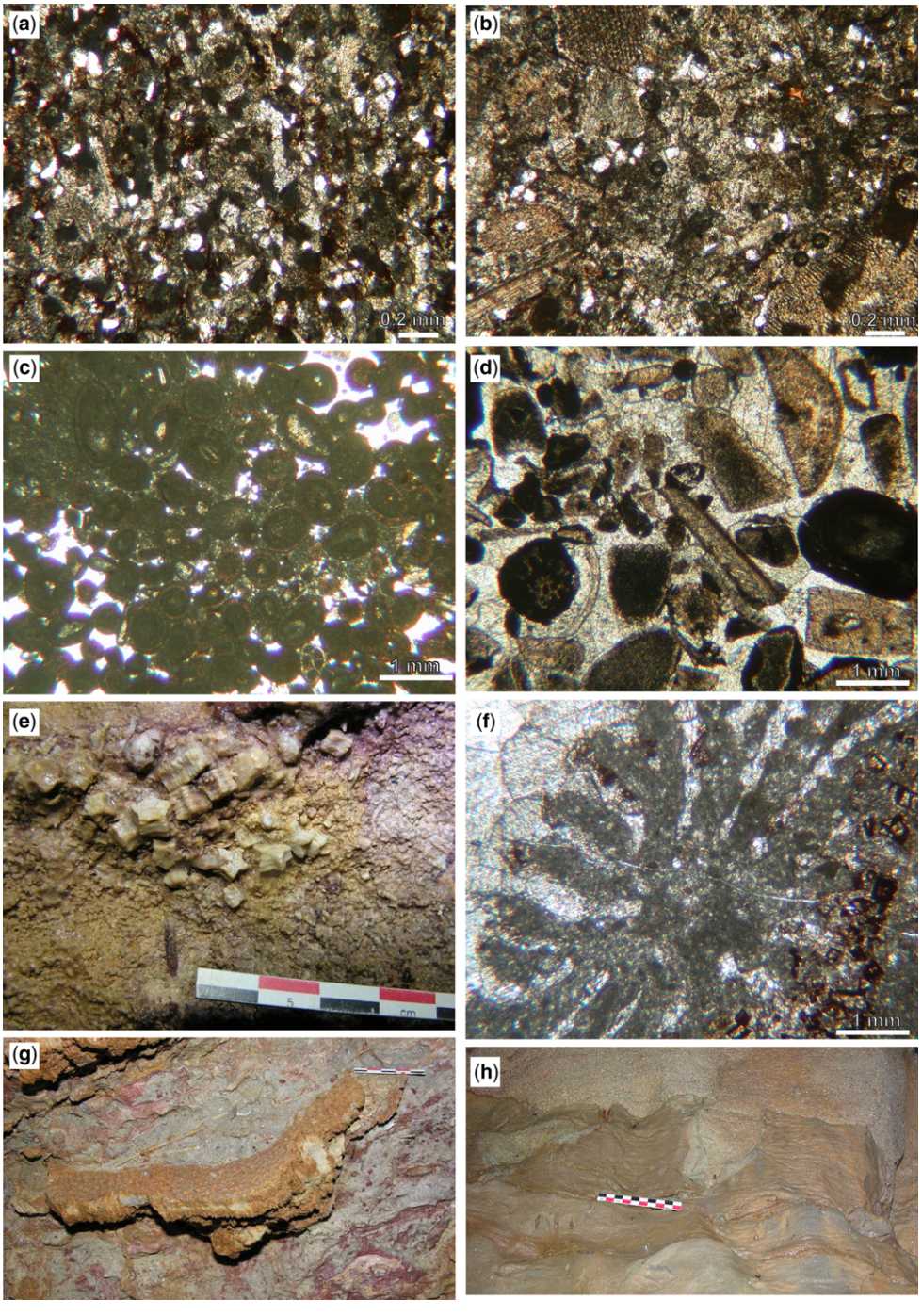

Fig. 4. (**a**) F2–F3 facies association, distal storm deposits. (**b**) F4–F5 facies association, proximal storm deposits. (**c**) F6–F7 facies association, oolitic tidal deposits. (**d**) F8 crinoidal limestone facies. (**e**) Preserved stalks from pentacrines, Calcaire à Entroques Formation, Grotte de la Rivière section. (**f**) F9–F10 reef facies association. (**g**) Silicified lamellar scleractinian colony from the Calcaire à Polypiers Member, Grotte de la Rivière section. (**h**) Subaerial exposure surface with palaeokarsts located at the top of the third sequence of the Calcaire à Polypiers Member, Grotte de la Rivière section (see * on Fig. 2).

cross-stratifications suggest high hydrodynamic conditions. The fauna, largely dominated by crinoids, associated with brachiopods, bivalves, gastropods, bryozoans and fragments of corals (Fig. 4d), emphasizes an open marine-shelf influence, associated with high rates of benthic *in situ* carbonate production and the proximity of reefal environments. The current ecological restrictions related to modern crinoids, and their extrapolations to Jurassic equivalents (Purser 1975; Benyahia 1982; Morestin 1986) suggest a necessity for normal salinity and oxygenation, good water limpidity, and an environment dominated by calm conditions in order to avoid the constant dislocation of organisms, and the presence of abundant plankton. The preservation of stalks (Fig. 4e) suggests a low transport rate of crinoids after their death.

An upper offshore environment, above the storm-wave base, periodically agitated and allowing only short-to-very-low transport of crinoid fragments, is inferred.

F9: bioclastic limestone, and F10: coral limestone. The bioclastic limestone and the coral limestone (Fig. 4f) are commonly interdigitated, suggesting that the coral reefs developed at depths of less than 100 m. The abundant micritic matrix, the presence of clay (Fig. 4g), the planar stratification and the upright position of the colonies suggest a calm and protected living environment for the coral limestone facies. The low angle of the reef flanks and the absence of reworked facies point to a biostromal geometry. The coral reefs are dominated by *Thamnasteria,* known to present various morphological shapes (Lathuilière 2000*b*), but inferred to have arisen in deeper environments than the large bioherms affected by fair-weather waves (Benyahia 1982; Morestin 1986; Piuz 2004). The annex-fauna, dominated by sea urchin spines, belemnites and bivalves exhibit the influence from the open-shelf. The very few crinoids emphasize a mutual exclusion with corals.

Facies 9 and 10 were deposited in a calm and protected depositional environment below the fair-weather base, most probably in the storm-wave zone.

MS

All the sections have relatively similar mean values (SGS, 0.36×10^{-8} m^3 kg^{-1}; Grotte Préhistorique, 0.64×10^{-8} m^3 kg^{-1}; Grotte de la Rivière, 0.86×10^{-8} m^3 kg^{-1}). These MS values are one order of magnitude lower than the $MS_{\text{marine standard}}$ of 5.5×10^{-8} m^3 kg^{-1} defined by Ellwood *et al.* (2011) on the basis of *c.* 11 000 marine rock samples, and our results indicate relatively pure carbonates in our sections.

When we compare MS behaviour with facies evolution, three types of behaviour are observed (Fig. 2):

(1) MS increases with shallowing-upward facies; we call this a positive correlation and it is the case for the Upper Bajocian of the SGS, Grotte Préhistorique and Grotte de la Rivière section, and a part of the Upper Aalenian/Lower Bajocian in the Grotte de la Rivière section (green arrows, Fig. 2).
(2) The MS decreases with shallowing facies; we call this a negative correlation and it is observed in the Lower Bathonian of the SGS, and of the Grotte Préhistorique sections (red arrows, Fig. 2).
(3) In the Lower Bajocian portion of the SGS and Grotte de la Rivière section, the link between MS and facies is not clear (uncertain correlation) and will be discussed further below (orange arrows, Fig. 2).

Sequential stratigraphy

The definition and terminology of depositional sequences derive from the Exxon model (e.g. Vail *et al.* 1991;Van Wagoner 1995; Catuneanu 2006) and are adapted to current knowledge of Jurassic sequential stratigraphy (e.g. Jacquin *et al.* 1998; Durlet & Thierry 2000; Hallam 2001). The second-order cycles (Fig. 2) are from Jacquin *et al.* (1998). The sequential stratigraphy of our sections relies on a combination of field work and the facies. The field work enabled us to identify unconformities (Figs 2 & 4h) and the geometry of the beds, and to establish the facies evolution. The facies and microfacies analyses have allowed us to develop two depositional models outlining the palaeoenvironmental and relative sea-level variations. Therefore, the vertical variations of relative sea level together with unconformities or abrupt shifts in palaeoenvironments allow several sedimentary cycles to be identified. The hierarchy of these cycles relies on the amplitude of palaeoenvironemental changes and the sequential background of the Bajocian and Bathonian of Burgundy (Jacquin *et al.* 1998; Durlet & Thierry 2000; Thiry-Bastien 2002). The contribution of MS towards this research goal is discussed later.

The Calcaire à Entroques Formation exhibits – in the SGS section at least – three complete shallowing-upward sequences (from crinoids meadows (F8) to biostrome depositional environments (F10), Fig. 2). At its base, a first incomplete sequence shows distal storm deposits (F2) grading vertically to a reefal environment (F10). In the Grotte de la Rivière section, the same sequences have also been identified at the base of the Calcaire à Entroques Formation (Fig. 2). However,

compared with a thickness of *c.* 20 m in SGS, they only reach 3 m of thickness in the Grotte de la Rivière. In addition, in the Grotte de la Rivière, the upper boundaries of the basal and third sequences are unconformity surfaces with subaerial exposure (Fig. 4h). These irregular surfaces develop at the top of the biostromes (F10 facies) and show decimetric palaeokarsts filled with crinoid limestones (F8 facies).

The Upper Bajocian of the SGS section registered palaeoenvironmental oscillations from the outer ramp (F1) to the top of the mid ramp (F5) (Fig. 2) and three complete depositional sequences were recognized. The first sequence postdating the Vesulian discontinuity reaches its maximum flooding surface at the first appearance of the F1 facies, at the base of unit 5 (Fig. 2) and ends with several proximal storm-dominated beds in the upper part of the *garantiana* Zone. The second sequence ends 2 m above the base of the lateral equivalent of the Marnes à *O. acuminata* Formation, in the lower part of the *parkinsoni* Zone. The third sequence ends in the Calcaires de Sermizelles Formation, in the uppermost part of the *parkinsoni* Zone. In the Grotte Préhistorique section, only the lateral third sequence is identified and correlated to the SGS section (Fig. 2). This sequence ends at the occurrence of the very proximal storm-influenced beds. The thickness of this lateral equivalent sequence is *c.* 15 m in SGS and 8 m in the Grotte Préhistorique. In both SGS and Grotte Préhistorique sections (Fig. 2), the last third-order trangressive cycle is expressed by a short retrograding phase, quickly evolving to an aggrading Bathonian oolitic sedimentation. The bathymetric amplitude of this maximum flooding surface might be reduced by the second-order regressive phase.

Discussion

Depositional model

The facies F1 to F7 are included in a first model (Fig. 3a), corresponding to a homoclinal carbonate ramp, including facies from the outer ramp to the inner ramp. This model represents the facies succession and ramp profile during the Upper Aalenian/Lower Bajocian (except the Calcaire à Entroques Formation) and during the Upper Bajocian to the Lower Bathonian (Fig. 2). Below the storm-wave base, the hemipelagic sedimentation is only affected by sparse distal storm deposits (F1) and includes most of the Marnes à *O. acuminata* Formation. In the mid ramp, the occurrence of thick proximal storm deposits towards the upper mid ramp increase accordingly to storm energy (F2 to F5). The common coquinas in the Calcaires de Sermizelles Formation of the Grotte Préhistorique section (Fig. 2) are in agreement with the facies developed by Pellenard *et al.* (1998). The inner ramp is dominated by the action of tide and fair-weather waves (Javaux 1992) leading to the development of an oolitic shoal and tidal flat (F6 and F7).

The second depositional model (Fig. 3b), applicable to the Lower Bajocian Calcaire à Entroques, showed a multiple-slopes geometry due to the development of bioherms, biostromes and a 'crinoids meadow' (facies F8 to F10). Although the exact palaeobathymetry significance of Bajocian crinoids accumulations is still debated (Neumeier 1998), the frequent interdigitating F9 and F10 facies in our sections and the low post-mortem transport of crinoids (Fig. 4e) suggest that the crinoids meadows should have developed nearby and in competition with the reefs. In agreement with Purser (1975), storm waves most probably reworked the crinoids along lines of higher hydrodynamic energy, developing sub-tidal bars of accumulations possibly parallel to the bioherms. In contrast to Daulin (1969) and Piuz (2004), but in agreement with Benyahia (1982), Morestin (1986) and Dromart *et al*. (1996), the biostromes (F10) are assumed to have developed in shallower environments than most of the crinoid meadows, and below the bioherms. These well-documented reefs (Benyahia 1982; Morestin 1986; Dromart *et al*. 1996) should have offered protection against storm-wave energy, and the biostromes would have benefited from an area of quiet hydrodynamic conditions in which clay accumulated, limiting crinoid expansion (F9). These settings, favouring colonization by pioneer biostromes, have been established through several studies (Daulin 1969; Purser 1975; Benyahia 1982; Piuz 2004), and are in agreement with our sections. On the Grotte de la Riviere section, the first lamellar coral colonies appear on the F2 facies (Fig. 2). These pioneer colonies were therefore most probably able to settle and develop on a loose substrate during periods of low sedimentation rate or after a storm (Piuz 2004), these being conditions that favour lateral instead of vertical growth (Lathuilière 2000*a*, *b*). In addition, a resistant greyish limestone included in the Calcaire à Entroques Formation has been described by Barusseau (1967) and Benyahia (1982) and is considered as having been formed in a calm area where no biostromes developed.

MS and facies

In our homoclinal carbonate ramp model, environments dominated by the tide and fair-weather waves (F6 and F7) show low negatives mean MS values. This is due to the constant and high water agitation during deposition that probably did not allow the deposition of siliciclastic particles. In

addition, the values decrease from the distal (F6) to the proximal (F7) facies. In the shallowest facies (F7), the very high carbonate production (ooïds production and many bioclasts) tends to decrease the MS values. Accordingly, in these settings, the regressions on the facies curve (Fig. 2) correlate with a decrease of the MS values, and the transgressions on the facies curve correlate with an increase of the MS values (red arrows, Fig. 2).

From the mid ramp towards outer ramp environments (F1 to F5) of the homoclinal carbonate ramp model, MS mean values are positive and low (Fig. 5a). This seems to be related to good carbonate productivity and to the ramp geometry. The occurrence of a well-developed oolitic shoal and/or tidal flat is expected to enhance the occurrence of a restricted environment that is protected from the open marine shelf. The siliciclastic magnetic minerals are partially retained in this restricted environment, most likely at the expense of the mid ramp environments. In addition, the mean MS values per facies (Fig. 5a) decrease towards the deeper environments. This pattern seems to be related to the effect of the vicinity of a landmass on the distribution of magnetic minerals. In addition, storms have been considered as significant suppliers of

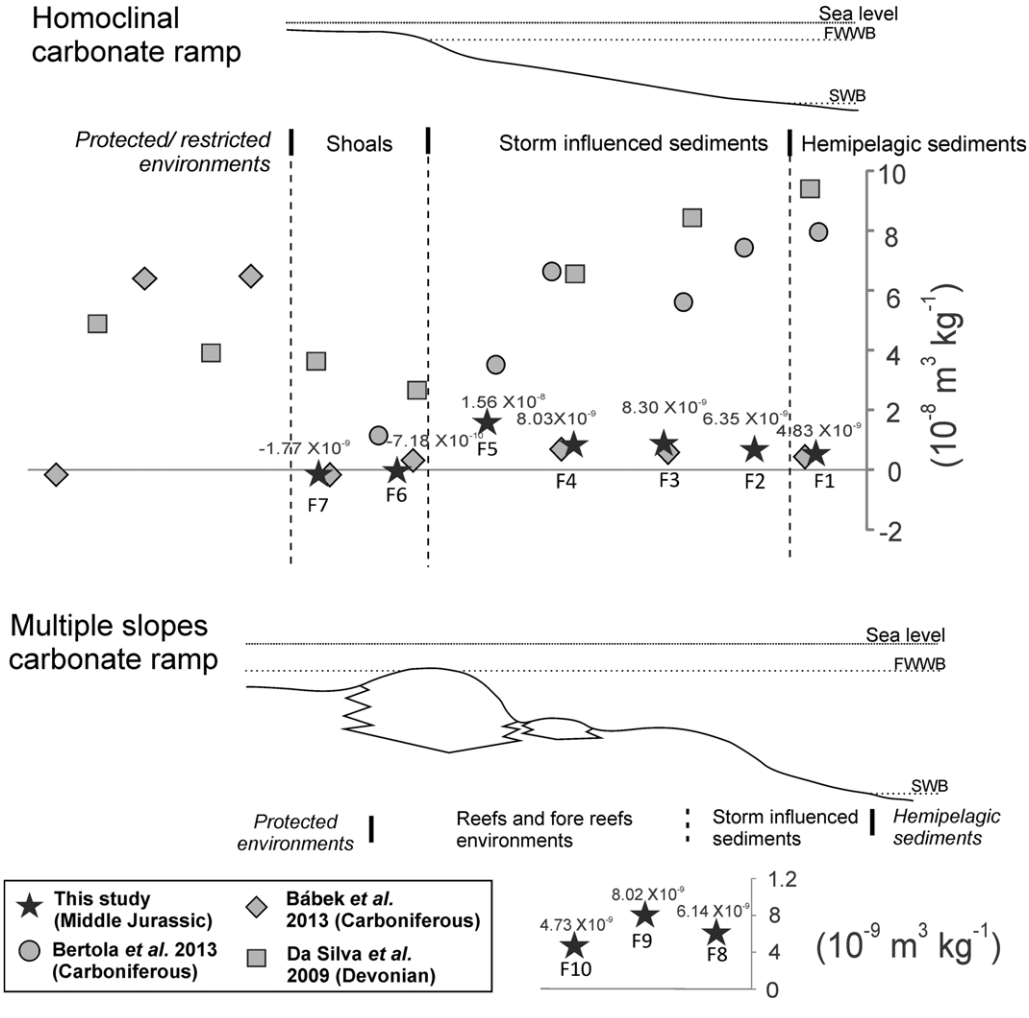

Fig. 5. Average values of bulk magnetic susceptibility per facies. (**a**) Facies of the homoclinal carbonated ramp. (**b**) Facies of the carbonate ramp with reef build-up. Values of the homoclinal ramp model are compared with values from Devonian and Carboniferous ramps showing similar sedimentary settings. FWWB, fair weather wave base; SWB, storm wave base.

siliciclastic magnetic minerals (Ellwood *et al.* 2001). The decrease of storm deposits towards the deeper environments (F5 to F1) could therefore favour the decrease of mean MS values towards the deeper environments. Consequently, in these settings, the regressions on the facies curve (Fig. 2) correlate with an increase of the MS values, and the transgressions on the facies curve correlate with a decrease of the MS values (green arrows, Fig. 2).

The reefal environments of the multiple-slopes carbonate ramp show lower average bulk MS values (Fig. 5b) than proximal storm deposits of the homoclinal carbonate ramp (Fig. 5a), although they share the same range of bathymetry (Fig. 3a, b). The higher *in situ* carbonate production of the reefal environments might have diluted the effect of the grains driving the magnetic signal. In these environments, no relationship appears between the mean MS values and the facies (Fig. 5b), and consequently, the relationship between sea-level variations and MS signal is unclear for the Calcaire à Entroques Formation (orange arrows, Fig. 2).

Therefore, unlike the lithological curves, the MS curve trends cannot be used as a direct proxy for palaeobathymetric variations in our sections. They are a function of the facies belt and prevailing depositional environment. The relationships established between the relative sea-level variations and MS signal are valuable because a relationship between a palaeoenvironmental proxy and MS values is a first indicator of a preserved primary signal (e.g. Da Silva & Boulvain 2002, 2006). Moreover, the MS signal trends can be used in the major part of our section to corroborate the sea-level variations deduced from the facies curves. During the Bajocian (except for the Calcaire à Entroques Formation), the regressions on the facies curve (Fig. 2) are coeval with an increase of the MS values, and the transgressions are coeval with a decrease of the MS values. During the Bathonian, the regressions on the facies curve (Fig. 2) are coeval with a decrease of the MS values, and the transgressions are coeval with an increase of the MS values.

The relationship between facies and MS on carbonate and ramp models has already been studied on the Tournaisian of China (Zhang *et al.* 2000) and Belgium (Bertola *et al.* 2013), on the Devonian of Belgium (Mabille & Boulvain 2007; Da Silva *et al.* 2009*a*) and Germany (Mabille *et al.* 2008), and on the Tournaisian and Early Visean in Western Europe (Bábek *et al.* 2010) and of South Whales (Bábek *et al.* 2013). On the Devonian carbonate platform (Da Silva *et al.* 2009*a*, *b*), the MS signal is influenced by siliciclastic input (e.g. Ellwood *et al.* 1999), with a decrease of MS values towards deeper facies. This is explained by the fact that deeper facies are away from the main source on the land. On the Devonian ramp (Da Silva *et al.* 2009*a*), the evolution is opposite with an increase of MS values from the inner to the outer ramp. This behaviour is explained through the influence of water agitation, sedimentation rate and/or carbonate production, controlling magnetic mineral distribution. In this Devonian example, and in contrast to our Jurassic values (Fig. 5a), the MS values are lowest in the mid ramp which is characterized by the highest carbonate productivity and water agitation during deposition. MS values are higher in the outer ramp, where water agitation and carbonate production are the lowest, allowing magnetic particles to settle out. Mabille *et al.* (2008) and Bertola *et al.* (2013) reached similar conclusions on the Devonian and Carboniferous of Belgium. Bábek *et al.* (2010) conclude that these trends are related to landward/basinward facies shifts of a low-productivity carbonate ramp. Bábek *et al.* (2013) noticed the same trend, with minimal values for the oolitic barrier, as in our Jurassic sections. They attribute these results mostly to the dilution of the terrigenous inputs by carbonates, in relation to carbonate production and carbonate dispersal.

Sequence stratigraphy

The Mid Cimmerian unconformity which predates a transgressive phase of a second-order cycle (Durlet & Thierry 2000) is not observed in our sections. Daulin (1969), Purser (1975) and Durlet & Thierry (2000) assumed that the tectonic uplift might have been of lower amplitude in the Mâconnais area, allowing the deposition of several depositional sequences during the Aalenian–Bajocian transition. According to Durlet & Thierry (2000), the geometry of the reef and its lateral variations during the *propiquans* and *humphriesianum* Zones of Lower Bajocian might highlight four regressive and transgressive trends due to third-order cycles, where the subaerial exposure surfaces indicate a temporary emersion of the reefs, such as at the top of the basal and third sequence of the Grotte de la Rivière (Fig. 4h). Despite a consequent thickness difference, the Calcaire à Polypiers Member shows at least three complete depositional sequences in both SGS and Grotte de la Rivière sections (Fig. 2). The identification of these sequences permits a precise correlation of our sections and allows their integration into the regional canvas. The difference of thickness seems to be related to the position of the sections along the reef, the Grotte de la Rivière section being in a more lateral position than the SGS section. The Vesulian disconformity is highlighted more by the sharp lithological and platform geometry transition than by an unconformity surface. The transition is identified in both the SGS and the Grotte de la Rivière section (VD on Fig. 2).

It is important to note that neither the SGS nor the Grotte de la Rivière reefal units rests on a thick bioclastic substratum. In the absence of new biostratigraphical data, it is difficult to be precise about the stratigraphical position of the base of the reefal lenses. The first hypothesis proposed is that the studied area was deeper than the average bathymetry in Mâconnais, and the various storm-dominated beds deposited below the reefal episodes are time-equivalent lateral variations of the Calcaire à Entroques Formation. The reefal lenses would have thus developed in the *propinquans* and *humphriesianum* ammonite Zones. The second hypothesis is that the Mid Cimmerian unconformity would have had very low impact in the studied area, and the transition from Aalenian storm-dominated sediments (Quesne *et al.* 2000) to Bajocian reefs would have been continuous, in the absence of thick crinoidal limestones in between. Such a transition has been described at Saint-Marc-sur-Seine, 140 km north of Azé (Durlet & Thierry 2000). In this case, the series could be condensed and the storm deposits below the reefal development would have been deposited in the Upper Aalenian. The first reefal lenses could therefore appear in the *discites* and *laeviscula* Zones, and then spread in the *propinquans* and *humphriesianum* Zones. This would explain the increasing thickness of coral beds at the expense of crinoids beds in the depositional sequences (Fig. 2), while in a general second-order transgressive phase (Jacquin *et al.* 1998).

The Upper Bajocian in Burgundy is subject to high tectonic activity inducing important individualizations of palaeogeographical areas, partly due to the reactivation of Hercynian faults (Graciansky *et al.* 1993; Pellenard *et al.* 1998) making large-scale correlations of the third-order sequences more difficult (Durlet & Thierry 2000). On the SGS and Grotte Préhistorique sections, the occurrence of a third-order maximum flooding surface at the base of the Marnes à *O. acuminata* Formation, and the maximum flooding surface of the third sequence in the Calcaires de Sermizelles is in agreement with Pellenard *et al.* (1998), while the first depositional sequence of the Upper Bajocian is uncorrelated (Fig. 2). This suggests a possible regional-scale sequential correlation, except for the lowest part of the Upper Bajocian. In the SGS and Grotte Préhistorique sections, the sequences based on the facies and MS positive and negative correlations might be showing more precise correlations than the lithostratigraphic framework (Fig. 2). Smaller variations of the facies curve, as in the Oolithe Blanche Formation of the SGS section, are identified (Fig. 2). These changes, often in relationship with the MS curve, are assumed to be related to fourth- or fifth-order sequences.

Conclusions

In this paper, we selected three Bajocian and Bathonian sections from the southeastern Paris Basin in the Mâconnais area (Burgundy, France), in order to provide a detailed sedimentological model, complemented by magnetic susceptibility (MS) analysis. The reference section of this work (Saint-Gengoux-de-Scissé (SGS) section) is exceptionally well preserved and continuous from Lower Bajocian to Bathonian. Ten facies were defined and grouped into six facies associations (external ramp, distal storm deposits, proximal storm deposits, inner ramp, crinoid meadows and coral reefs). Two sedimentological models were proposed to identify and assess the palaeoenvironmental dynamics occurring during the Bajocian and lower Bathonian in the Mâconnais area. The first model is of a homoclinal carbonate ramp with storm deposits and shallower oolitic shoals. The second model is of a multiple-slopes carbonate ramp with reef complexes which developed during a short time interval in the Lower Bajocian. The bulk MS signal has been shown to be partially related to both facies and ramp geometry. Its relationship to facies is mainly related to carbonate productivity: oolitic and reefal facies, characterized by the highest carbonate production and water agitation during deposition, display the lowest values. The storm deposits show higher values, suggesting that the MS values are driven by the siliciclastic inputs. These detrital inputs are distributed in accordance with the general ramp geometry and the hydrodynamic conditions. In the homoclinal carbonate ramp, mean MS values per facies decrease from upper to lower mid ramp and increase from the upper to lower inner ramp. These trends allow the use of MS trends as a complementary palaeobathymetric tool in those sedimentary settings. Based on facies and MS curves in the proper sedimentary environments, ten complete third-order sequences have been identified. These provide a sequential canvas which improve upon the stratigraphic precision of the studied area, previously based on the lithofacies framework, and permit a regional correlation. MS has proved to be a complementary proxy of great interest for palaeoenvironmental interpretation, correlations and sequential stratigraphy for the Bajocian and Bathonian of the southeastern Paris Basin.

This work has been financially supported by University of Liège and the Institut de Recherche du Mâconnais, Val de Saône. Improvements have been applied during work for the PhD thesis of Sylvain Dechamps, financially supported by a grant of the Fonds National de la Recherche (FNR) of Luxembourg. We wish to thank the town council of Azé and the Conseil Général de Saône-et-Loire for access to the caves. Special thanks are given to the Cultural Association of the Azé caves, and particularly to Lionel and Johan

Barriquand for their logistics support, their help in the field, and their advice. This paper is part of the IGCP-580 programme 'Application of MS as a palaeoenvironmental proxy'.

References

Bábek, O., Kalvoda, J., Aretz, M., Cossey, P. J., Devuyst, F.-X., Herbig, H.-G. & Sevastopulo, G. 2010. The correlation potential of magnetic susceptibility and outcrop gamma-ray logs at Tournaisian-Viséan boundary sections in Western Europe. *Geologica Belgica*, **13**, 291–308.

Bábek, O., Kalvoda, J., Cossey, P. J., Šimíček, D., Devuyst, F.-X. & Hargreaves, S. 2013. Facies and petrophysical signature of the Tournaisian/Viséan (Lower Carboniferous) sea-level cycle in carbonate ramp to basinal settings of the Wales-Brabant massif, British Isles. *Sedimentary Geology*, **284–285**, 197–213.

Barriquand, J. & Barriquand, L. 2000. *Rapport et bilan annuel*. Fouille programmée 2000. Galerie des Aiglons, Grotte Préhistorique d'Azé (Saône-et-Loire). Service Régional de l'Archéologie, Dijon.

Barriquand, J. & Barriquand, L. 2001. *Rapport et bilan annuel*. Fouille programmée 2001. Galerie des Aiglons, Grotte Préhistorique d'Azé (Saône-et-Loire). Service Régional de l'Archéologie, Dijon.

Barriquand, J. & Barriquand, L. 2009. Azé 1-4 (Saône-et-Loire, Burgundy, France): its position in the filling up of the cave and the conditions under which it was put in place. *Slovenský kras, Acta Carsologica Slovaca*, **47**, 105–112.

Barriquand, J., Barriquand, L., Quinif, Y. & Argant, A. 2006. Grottes d'Azé (Saône-et-Loire, France) – Bilan et interprétation des datations U/Th. *Geologica Belgica*, **9/3–4**, 309–321.

Barusseau, M. 1967. *Les changements de faciès du Jurassique moyen dans les Monts du Mâconnais*. Laboratoire de l'école normale supérieure de géologie, Paris, **1**.

Benyahia, M. 1982. *Les séries sédimentaires d'âge aalénien moyen-bajocien supérieur dans les chaînons du Mâconnais: organisation et évolution des environnements bio-sédimentaires*. PhD thesis, Université de Dijon, Dijon.

Berger, S. & Martin, J. 1995. *Grottes d'Azé: étude stratigraphique et lithologie*. License thesis, Université de Dijon.

Bertola, C., Boulvain, F., Da Silva, A.-C. & Poty, E. 2013. Sedimentology and magnetic susceptibility of Mississipian (Tournaisian) carbonate sections in Belgium. *Bulletin of Geosciences, Czech Geological Survey, Prague*, **88**, 69–82.

Boulila, S., Hinnov, L. A. *et al.* 2008. Astronomical calibration of the Early Oxfordian (Vocontian and Paris basins, France): consequences of revising the Late Jurassic time scale. *Earth and Planetary Science Letters*, **276**, 40–51.

Boulila, S., De Rafélis, M., Hinnov, L. A., Gardin, S., Galbrun, B. & Collin, P.-Y. 2010. Orbitally forced climate and sea-level changes in the Paleoceanic Tethyan domain (marl–limestone alternations, Lower Kimmeridgian, SE France). *Palaeogeography, Palaeoclimatology, Palaeoecology*, **292**, 57–70.

Boulvain, F., Da Silva, A.-C., Mabille, C., Hladil, J., Gersl, M., Koptikova, L. & Schnabl, P. 2010. Magnetic susceptibility correlation of km-thick Eifelian-Frasnian sections (Ardennes and Moravia). *Geologica Belgica*, **13**, 309–318.

Brigaud, B., Durlet, C., Deconinck, J.-F., Vincent, B., Pucéat, E., Thierry, J. & Trouiller, A. 2009. Facies and climate/environmental changes recorded on a carbonate ramp: a sedimentological and geochemical approach on Middle Jurassic carbonates (Paris Basin, France). *Sedimentary Geology*, **222**, 181–206.

Burchette, T. P. & Wright, V. P. 1992. Carbonate ramp depositional systems. *Sedimentary Geology*, **79**, 3–57.

Catuneanu, O. 2006. *Principles of Sequence Stratigraphy*. Elsevier, Amsterdam.

Combier, J., Gaillard, C. & Moncel, M.-H. 2000. L'industrie du Paléolithique inférieur de la Grotte d'Azé (Saône-et-Loire - Azé 1-1). *Bulletin de la Société Préhistorique Française*, **7**, 349–370.

Contini, D. & Mangold, C. 1980. Évolution paléogéographique de la France au Jurassique moyen. *In*: Debrand-Passard, S., Courbouleix, S. & & Lienhardt, M. J. (eds) *Synthèse géologique du Sud-Est de la France*. Mémoires du BRGM, France, **125**, 218–221.

Coulon, M. 1979. *Les systèmes biosédimentaires en relation avec les calcaires à entroques de Bourgogne (Stratigraphie – Sédimentologie – Géochimie)*. PhD thesis, Dijon.

Crick, R. E., Ellwood, B. B., El Hassani, A., Feist, R. & Hlalil, J. 1997. MagnetoSusceptibility Event and Cyclostratigraphy (MSEQ of the Eifelian- Givetian GSSP and associated boundary sequences in north Africa and Europe. *Episodes*, **20**, 167–175.

Crick, R. E., Ellwood, B. B., El Hassani, A. & Feist, R. 2000. Proposed magnetostratigraphy susceptibility magnetostratotype for the Eifelian–Givetian GSSP (Anti-Atlas, Morocco). *Episodes*, **23**, 93–101.

Crick, R. E., Ellwood, B. B., Hladil, J., El Hassani, A., Hrouda, F. & Chlupac, I. 2001. Magnetostratigraphy susceptibility of the Pridolian–Lochkovian (Silurian–Devonian) GSSP (Klonk, Czech Republic) and coeval sequence in Anti-Atlas Morocco. *Palaeogeography, Palaeoclimatology, Palaeoecology*, **167**, 73–100.

Crick, R. E., Ellwood, B. B. *et al.* 2002. Magnetostratigraphy susceptibility of the Frasnian/Famennian boundary. *Palaeogeography, Palaeoclimatology, Palaeoecology*, **181**, 67–90.

Da Silva, A. C. & Boulvain, F. 2002. Sedimentology, magnetic susceptibility and isotopes of a Middle Frasnian carbonate platform: Tailfer section, Belgium. *Facies*, **46**, 89–102.

Da Silva, A. C. & Boulvain, F. 2003. Sedimentology, magnetic susceptibility and correlations of Middle Frasnian platform limestone (Tailfer and Aywaille sections, Belgium). *Geologica Belgica*, **6**, 81–96.

Da Silva, A. C. & Boulvain, F. 2006. Upper Devonian carbonate platform correlations and sea level variations recorded in magnetic susceptibility. *Palaeogeography, Palaeoclimatology, Palaeoecology*, **240**, 373–388.

Da Silva, A. C. & Boulvain, F. 2010. Magnetic susceptibility, correlations and Paleozoic environments: foreword. *Geologica Belgica*, **13**, 287–290.

Da Silva, A. C., Mabille, C. & Boulvain, F. 2009*a*. Influence of sedimentary setting on the use of magnetic susceptibility: examples from the Devonian of Belgium. *Sedimentology*, **56**, 1292–1306.

Da Silva, A. C., Potma, K., Weissenberger, J. A. W., Whalen, M. T., Humblet, M., Mabille, C. & Boulvain, F. 2009*b*. Magnetic susceptibility evolution and sedimentary environments on carbonate platform sediments and atolls, comparison of the Frasnian from Belgium and Alberta, Canada. *Sedimentary Geology*, **214**, 3–18.

Da Silva, A. C., Yans, J. & Boulvain, F. 2010. Early-middle Frasnian (early Late Devonian) sedimentology and magnetic susceptibility of the Ardennes area (Belgium): identification of severe and rapid sea-level fluctuations. *Geologica Belgica*, **13**, 319–332.

Da Silva, A. C., De Vleeschouwer, D. *et al.* 2013. Magnetic susceptibility as a high-resolution correlation tool and as a climatic proxy in Paleozoic rocks - merits and pitfalls: examples from the Devonian in Belgium. *Marine and Petroleum Geology*, **46**, 173–189.

Daulin, J.-L. 1969. *Les calcaires du Bajocien de Bourgogne, stratigraphie, sédimentologie*. PhD thesis, Faculté de Dijon, Dijon.

Dera, G., Brigaud, B. *et al.* 2011. Climatic ups and downs in a disturbed Jurassic world. *Geology*, **39**, 215–218.

Dercourt, J., Ricou, L. E. & Vrielynck, B. 1993. *Atlas Tethys Palaeoenvironmental Maps*. Gauthier-Villars, Paris.

Devleeschouwer, X. 1999. *La transition Frasnien–Famennien (Dévonien Supérieur) en Europe: Sédimentologie, stratigraphie séquentielle et susceptibilité magnétique*. PhD thesis, Université Libre de Bruxelles, Brussels.

De Vleeschouwer, D., Da Silva, A. C., Boulvain, F., Crucifix, M. & Claeys, P. 2012*a*. Precessional and half-precessional climate forcing of Mid-Devonian monsoonlike dynamics. *Climate of the Past*, **7**, 1427–1455.

De Vleeschouwer, D., Whalen, M. T., Day, J. E. & Claeys, P. 2012*b*. Cyclostratigraphic calibration of the Frasnian (Late Devonian) time scale (western Alberta, Canada). *Geological Society of America Bulletin*, **124**, 928–942.

Dromart, G., Allemand, P., Garcia, J.-P. & Robin, C. 1996. Variation cyclique de la production carbonatée au Jurassique le long d'un transect Bourgogne-Ardèche, Est-France. *Bulletin de la Société Géologique de France*, **167**, 423–433.

Dunham, R. J. 1962. Classification of carbonate rocks according to depositional texture. *In*: Ham, W. E. (ed.) *Classification of Carbonate Rocks*. American Association of Petroleum Geologists, Tulsa, Memoirs, **1**, 108–121.

Durlet, C. 1996. *Apport de la diagenèse des discontinuités à l'interprétation paléo-environnementale et séquentielle d'une plate-forme carbonatée. Exemple des Calcaires à entroques du Seuil de Bourgogne (Aalénien-Bajocien)*. PhD thesis, Bourgogne.

Durlet, C. & Thierry, J. 2000. Modalités séquentielles de la transgression aaléno-bajocienne sur le sud-est du Bassin parisien. *Bulletin de la Société géologique de France*, **171**, 327–339.

Durlet, C., Jacquin, T. & Floquet, M. 1997. Tectonique synsédimentaire distensive dans les calcaires aaléno-bajociens du seuil de Bourgogne. *Comptes Rendus de l'Académie des Sciences, Paris, France*, **324**, 1001–1004.

Ellwood, B. B., Crick, R. E. & El Hassani, A. 1999. Magnetosusceptibility event and cyclostratigraphy (MSEC) method used in geological correlation of Devonian rocks from Anti-Atlas Morocco. *American Association of Petroleum Geologists*, **83**, 1119–1134.

Ellwood, B. B., Crick, R. E., El Hassani, A., Benoist, S. L. & Young, , R. H. 2000. Magnetosusceptibility event and cyclostratigraphy method applied to marine rocks: detrital input v. carbonate productivity. *Geology*, **28**, 1135–1138.

Ellwood, B. B., Crick, R. E., Carcia-Alcade Fernandez, J. L., Soto, F. M., Truyóls-Massoni, M., El Hassani, A. & Kovas, E. J. 2001. Global correlation using magnetic susceptibility data from Lower Devonian rocks. *Geology*, **29**, 583–586.

Ellwood, B. B., Garcia-Alcalde, J. L. *et al.* 2006. Stratigraphy of the Middle Devonian boundary: formal definition of the susceptibility magnetostratotype in Germany with comparisons to sections in the Czech Republic, Morocco and Spain. *Tectonophysics*, **418**, 31–49.

Ellwood, B. B., Carlton, E. B. & MacDonald, W. D. 2007. Magnetostratigraphy susceptibility of the Upper Ordovician Kope Formation, northern Kentucky. *Palaeogeography, Palaeoclimatology, Palaeoecology*, **243**, 42–54.

Ellwood, B. B., Tomkin, J. H. *et al.* 2011. A climate-driven model and development of a floating point time scale for the entire Middle Devonian Givetian Stage: a test using magnetostratigraphy susceptibility as a climate proxy. *Palaeogeography, Palaeoclimatology, Palaeoecology*, **304**, 85–95.

Ellwood, B. B., Lambert, L. L., Tomkin, J. H., Bell, G. L., Nestell, M. K., Nestell, G. P. & Wardlaw, B. R. 2012. Magnetostratigraphy susceptibility for the Guadalupian series GSSPs (Middle Permian) in Guadalupe Mountains National Park and adjacent areas in West Texas. *In*: Jovane, L., Herrero-Bervera, E., Hinnov, L. A. & & Housen, B. A. (eds) *Magnetic Methods and the Timing of Geological Processes*. Geological Society, London, Special Publications, **373**, 375–394, http://dx.doi.org/10.1144/SP373.1

Ellwood, B. B., Wang, W.-H., Tomkin, J. H., Kenneth, T. R., El Hassani, A. & Wright, A. M. 2013. Testing high resolution magnetic susceptibility and gamma radiation methods in the Cenomanian–Turonian (Upper Cretaceous) GSSP and near-by coeval section. *Palaeogeography, Palaeoclimatology, Palaeoecology*, **378**, 75–90.

Enay, R. & Mangold, C. 1980. Synthèse paléogéographique du Jurassique français, Document du Laboratoire de Géologie de Lyon. *Groupe Français d'Etude du Jurassique*, **5**, 220.

Ferry, S., Pellenard, P.-E. *et al.* 2007. Synthesis of recent stratigraphic data on Bathonian to Oxfordian deposits of the eastern Paris Basin. *In*: Lebon, P.

(ed.) *A Multi-Disciplinary Approach to the Eastern Jurassic Border of the Paris Basin (Meuse/Haute-Marne)*. ANDRA, Agence nationale pour la gestion des déchets radioactifs. Mémoires de la Société Géologique de France, Chatenay-Malabry, France. Nouvelle Série. **178**, 37–57.

Floquet, M., Laurin, B., Laville, P., Marchand, D., Menot, J. C. & Thierry, J. 1989. Les systèmes sédimentaires bourguignons d'âge Bathonien terminal-Callovien. *Bulletin du centre de recherches elf exploration production Elf-Aquitaine*, **13**, 133–165.

Gibbs, M. T., Bluth, G. J. S., Fawcett, P. J. & Kump, L. R. 1999. Global chemical erosion over the last 250 my: variations due to changes in paleogeography, paleoclimate, and paleogeology. *American Journal of Science*, **299**, 611–651.

Graciansky, P.-C. de, Dardeau, G., Dumont, T., Jacquin, T., Marchand, D., Mouterde, R. & Vail, P. 1993. Depositional sequence cycles, transgressive-regressive facies-cycles, and extensional tectonics: example from the southern Subalpine Jurassic basin, France. *Bulletin de la Société Géologique de France*, **164**, 709–718.

Hallam, A. 2001. A review of the broad pattern of Jurassic sea-level changes and their possible causes in the light of current knowledge. *Palaeogeography, Palaeoclimatology, Palaeoecology*, **167**, 23–37.

Hesselbo, S. P., Morgans-Bell, H. S., Mcelwain, J. C., Rees, P. M., Robinson, S. A. & Ross, C. E. 2003. Carbon-cycle perturbation in the Middle Jurassic and accompanying changes in the terrestrial paleoenvironment. *The Journal of Geology*, **111**, 259–276.

Hladil, J., Bosak, P., Slavik, L., Carew, J. L., Mylroie, J. E. & Gersl, M. 2003. Early diagenetic origin and persistence of gamma-ray and magnetosusceptibility patterns in platform carbonates: comparison of Devonian and Quaternary sections. *Physics and Chemistry of the Earth*, **28**, 719–727.

Hladil, J., Gersl, M., Strnad, L., Frana, J., Langrova, A. & Spisiak, J. 2005. Stratigraphic variation of complex impurities in platform limestones and possible significance of atmospheric dust: a study with emphasis on gamma-ray spectrometry and magnetic susceptibility outcrop logging (Eifelian–Frasnian, Moravia, Czech Republic). *International Journal of Earth Sciences*, **95**, 703–723.

Jacquin, T., Dardeau, G., Durlet, C. & Graciansky, P.-C. de 1998. The North Sea cycle: an overview of 2nd-order trangressive/regressive facies cycle in Western Europe. *In*: Graciansky, P.-C. de, Hardenbol, J., Jacquin, T. & Vail, P.-R. (eds) *Mesozoic and Cenozoic Sequence Stratigraphy of European Basins*. SEPM (Society for Sedimentary Geology), Tulsa, Oklahoma, USA. SEPM special publications, **60**,

Javaux, C. 1992. *La plate-forme parisienne et bourguignonne au Bathonien terminal et au Callovien—Dynamique sédimentaire, séquentielle et diagénétique, Place et creation des réservoirs potentiels*. Mémoires géologiques de l'Université de Dijon, Dijon, **16**, 1–342.

Koptíková, L. 2011. Precise position of the Basal Chotec event and evolution of sedimentary environments near the Lower-Middle Devonian boundary: the magnetic susceptibility, gamma-ray spectrometric, lithological, and geochemical record of the Prague Synform (Czech Republic). *Palaeogeography, Palaeoclimatology, Palaeoecology*, **304**, 96–112.

Lathuilière, B. 2000*a*. Coraux constructeurs du Bajocien inférieur de France. [Reef building corals of Lower Bajocian of France. Part 1.]. *GEOBIOS*, **33**, 51–72.

Lathuilière, B. 2000*b*. Coraux constructeurs du Bajocien inférieur de France. [Reef building corals of Lower Bajocian of France. Part 2.]. *GEOBIOS*, **33**, 153–181.

Lathuilière, B. & Marchal, D. 2009. Extinction, survival and recovery of corals from the Triassic to Middle Jurassic time. *Terra Nova*, **21**, 57–66.

Mabille, C. & Boulvain, F. 2007. Sedimentology and magnetic susceptibility of the Upper Eifelian–Lower Givetian (Middle Devonian) in SW Belgium : insights into carbonate platform initiation. *In*: Alvaro, J. J., Aretz, M., Boulvain, F., Munnecke, A., Vachard, D. & Vennin, E. (eds) *Palaeozoic Reefs and Bioaccumulations. Climatic and Evolutionary Controls*. Geological Society, London, Special Publications, **275**, 109–123, http://dx.doi.org/10.1144/GSL.SP.2007.275.01.08

Mabille, C., Pas, D., Aretz, M., Boulvain, F., Schröder, S. & Da Silva, A.-C. 2008. Deposition within the vicinity of the Mid-Eifelian High: detailed sedimentological study and magnetic susceptibility of a mixed ramp-related system from the Eifelian Lauch and Nohn formations (Devonian; Ohlesberg, Eifel, Germany). *Facies*, **54**, 597–612.

Morestin, B. 1986. *Sédimentation et diagenèse dans les «calcaires à entroques» de Bourgogne (France) (Aalénien – Bajocien)*. PhD thesis, Centre des sciences de la Terre, Université de Bourgogne.

Neumeier, U. 1998. Tidal dunes and sand waves in deep outer-shelf environments, Bajocian, Se Jura, France. *Journal of Sedimentary Research*, **68**, 507–514.

Pellenard, P.-E., Thiry-Bastien, P., Thierry, J. & Vincent, B. 1998. Approche sédimentologique du Bajocien supérieur-Bathonien inférieur du nord-ouest de la Bourgogne (sud-est du bassin de Paris): dynamique sédimentaire et reconstitution paléogéographique d'un secteur d'une plateforme carbonatée péri-téthysienne. *Géologie de la France*, **1**, 21–38.

Perthuisot, J. P. 1966. Contribution à l'étude géologique des Monts du Mâconnais (feuilles Tournus n°5 et Tournus n°6). *École normale supérieure, laboratoire de géologie, Paris*, **2**, 108.

Piuz, A.-D. 2004. *Micropaléontologie d'une plateforme bioclastique échinodermique : les calcaires à entroques du Bajocien du Jura méridional et de Bourgogne*. PhD thesis, Université de Genève.

Purser, B. H. 1975. *Sédimentation et diagenèse précoce des séries carbonatées du Jurassique moyen de Bourgogne*. PhD thesis. Université de Paris Sud, Orsay.

Quesne, D., Guiraud, M., Garcia, J.-P., Thierry, J., Lathuilière, B. & Audebert, N. 2000. Marqueurs d'une structuration extensive jurassique en arrière de la marge nord-téthysienne (monts du Mâconnais, Bourgogne, France). *Comptes Rendus de l'Académie des Sciences, Science de la Terre et des planètes/Earth and Planetary Sciences*, **330**, 623–629.

Racki, G., Racka, M., Matyja, H. & Devleeschouwer, X. 2002. The Frasnian/Famennian boundary interval in the South Polish–Moravian shelf basins: integrated

event stratigraphical approach. *Palaeogeography, Palaeoclimatology, Palaeoecology*, **181**, 251–297.

RAT, P., COUREL, L. *ET AL*. 1986. *Bourgogne Morvan*. 2nd edn. Guides géologiques régionaux, Masson, Paris, France.

THIERRY, J. 2000. Late Sinemurian, Middle Toarcian, Middle Callovian, Early Kimmeridgian, Early Tithonian. *In*: CRASQUIN, S. (ed.) *Atlas Peri-Tethys, Palaeogeographical Maps—Explanatory Notes*. CCGM/CGMW Edit, Paris, 49–110.

THIRY-BASTIEN, P. 2002. *Stratigraphie séquentielle des calcaires bajociens de l'est de la France: Jura-Bassin de Paris*. PhD thesis, Lyon.

TINTANT, H. 1963. Observations stratigraphiques sur le Jurassique moyen de Côte-d'Or. *Bulletin Scientifique de Bourgogne*, **21**, 93–117.

TUCKER, M. E. & WRIGHT, V. P. 1990. *Carbonate Sedimentology*. Blackwell Scientific Publications, Oxford.

VAIL, P. R., AUDEMARD, F., BOWMAN, S. A., EISNER, P. N. & PEREZ-CRUZ, C. 1991. The stratigraphic signatures of tectonics, eustasy and sedimentology: an overview. *In*: EINSELE, G., RICKEN, W. & SEILACHER, A. (eds) *Cycles and Events in Stratigraphy*. Springer-Verlag, Berlin, 617–659.

VAN WAGONER, J. C. 1995. Sequence stratigraphy and marine to nonmarine facies architecture of foreland basin strata, Book Cliffs, Utah, U.S.A. *In*: VAN WAGONER, J. C. & BERTRAM, G. T. (eds) *Sequence Stratigraphy of Foreland Basin Deposits; Outcrop and Subsurface Examples from the Cretaceous of North America*. American Association of Petroleum Geologists, Memoir, **64**, 9–21.

VINCENT, B., EMMANUEL, L., LOREAU, J.-P. & THIERRY, J. 1997. Caractérisation et interprétation de cycles géochimiques sur la plateforme bourguignonne (France) au Bajocien-Bathonien. *Comptes Rendus de l'Académie des Sciences, Science de la Terre et des planètes/Earth and Planetary Sciences*, **325**, 783–789.

WHALEN, M. T. & DAY, J. E. 2008. Magnetic susceptibility, biostratigraphy, and sequence stratigraphy: insights into Devonian carbonate platform development and basin infilling, western Alberta, Canada. *Society for Sedimentary Geology*, **89**, 291–314.

WHALEN, M. T. & DAY, J. 2010. Cross-basin variations in magnetic susceptibility influenced by changing sea level, paleogeography, and paleoclimate: upper Devonian, Western Canada. *Journal of Sedimentary Research*, **80**, 1109–1127.

ZHANG, S., WANG, X. & ZHU, H. 2000. Magnetic susceptibility variations of carbonates controlled by sea level changes – examples in Devonian to Carboniferous strata in southern Guizhou Province, China. *Science China D*, **43**, 266–276.

ZIEGLER, P. A. 1988. Evolution of the Arctic-North Atlantic and the Western Tethys. *American Association of Petroleum Geologists, Memoir*, **43**, 198, Tulsa, USA.